View metadata, citation and similar papers at core.ac.uk

brought to you by CORE

provided by ScholarWorks@UMass Amherst

University of Massachusetts Amherst
ScholarWorks@UMass Amherst

Chemical Engineering Faculty Publication Series | Chemical Engineering

2013

PEG-Phosphorylcholine Hydrogels As Tunable and Versatile Platforms for Mechanobiology

William G. Herrick
University of Massachusetts - Amherst

Thuy V. Nguyen
University of Massachusetts Amherst

Marianne Sleiman
University of Massachusetts Amherst

Samantha McRae
University of Massachusetts Amherst

Todd Emrick
University of Massachusetts Amherst

See next page for additional authors

Follow this and additional works at: https://scholarworks.umass.edu/che_faculty_pubs


Part of the Chemical Engineering Commons

Recommended Citation

Herrick, William G.; Nguyen, Thuy V.; Sleiman, Marianne; McRae, Samantha; Emrick, Todd; and Peyton, Shelly, "PEG-Phosphorylcholine Hydrogels As Tunable and Versatile Platforms for Mechanobiology" (2013). *Biomacromolecules*. 846.
https://doi.org/10.1021/bm400418g

This Article is brought to you for free and open access by the Chemical Engineering at ScholarWorks@UMass Amherst. It has been accepted for inclusion in Chemical Engineering Faculty Publication Series by an authorized administrator of ScholarWorks@UMass Amherst. For more information, please contact scholarworks@library.umass.edu.

Authors
William G. Herrick, Thuy V. Nguyen, Marianne Sleiman, Samantha McRae, Todd Emrick, and Shelly Peyton

This article is available at ScholarWorks@UMass Amherst: https://scholarworks.umass.edu/che_faculty_pubs/846

PEG-phosphorylcholine hydrogels as tunable and versatile platforms for mechanobiology

Running Title

PEG-phosphorylcholine hydrogels

William G. Herrick[1,2], Thuy V. Nguyen[1,2], Marianne Sleiman[1], Samantha McRae[3], Todd S. Emrick[3,4], and Shelly R. Peyton*[1,2,4,5]

*Corresponding Author

1. Department of Chemical Engineering
2. Institute for Cellular Engineering
3. Department of Polymer Science and Engineering
4. Materials Research Science and Engineering Center
5. Molecular and Cellular Biology Graduate Program

University of Massachusetts

Amherst, MA 01003

ABSTRACT

We report here the synthesis of a new class of hydrogels with an extremely wide range of mechanical properties suitable for cell studies. Mechanobiology has emerged as an important field in bioengineering, in part due to the development of synthetic polymer gels and fibrous protein biomaterials to control and quantify how cells sense and respond to mechanical forces in their microenvironment. To address the problem of limited availability of biomaterials, both in terms of mechanical range and optical clarity, we have prepared hydrogels that combine poly(ethylene glycol) (PEG), and phosphorylcholine (PC) zwitterions. Our goal was to create a hydrogel platform that exceeds the range of Young's moduli reported for similar hydrogels, while being simple to synthesize and manipulate. The Young's modulus of these "PEG-PC" hydrogels can be tuned over four orders of magnitude, much greater than commonly used hydrogels such as PEG-diacrylate, PEG–dimethacrylate, and polyacrylamide, with smaller average mesh sizes, and optical clarity. We prepared PEG-PC hydrogels to study how substrate mechanical properties influence cell morphology, focal adhesion structure, and proliferation across multiple mammalian cell lines, as a proof of concept. These novel PEG-PC biomaterials represent a new and useful class of mechanically tunable hydrogels for mechanobiology.

KEYWORDS

Poly(ethylene glycol), phosphorylcholine, hydrogel, mechanobiology, cell proliferation

INTRODUCTION

The development of tunable biomaterials has driven rapid progress in tissue engineering, either to facilitate or enhance the natural wound healing process, or to act as functional replacement tissues in the human body. Biomaterial platforms have been developed both for eventual *in vivo* application, as well as for *in vitro* model systems for studying complex biological processes, including cell migration, adhesion, proliferation, and differentiation. Information from these *in vitro* studies drives the design of implantable scaffolds, and promotes understanding of complex biology in environments more physiologically relevant than traditional plastic and glass surfaces. Studying cellular phenomenology and signaling mechanisms in microenvironments that capture key features of the *in vivo* extracellular matrix (ECM) is more efficient and cost-effective than animal studies, and may prove to be more predictive of human clinical outcome.

Mechanical cues from materials and the microenvironment, such as substrate modulus, shear stress, and stretch, influence cell migration,[1–3] differentiation,[4–6] and proliferation[7] (for review, see ref.[8]). Mechanotransduction, the translation of a mechanical cue from the ECM into a biochemical one, is mediated by focal adhesions.[9] There have been many studies on the effects of substrate modulus on cell spreading,[3,10–16] focal adhesion properties,[3,11,15,17] proliferation,[5,6,11,18–20] migration,[1–3,21,22] and phenotype and differentiation,[4,5,20,23–25] with several materials platforms.[3,12–14,18,20,26–29] Materials most commonly used to investigate mechanobiology are hydrogels, including synthetic polymers, such as polyacrylamide (PAA),[30–32] and poly(ethylene glycol) (PEG),[5] and biologically derived gels, such as alginate,[33] Matrigel™,[34] fibrin,[35] hyaluronic acid[14,20,29] and type I collagen.[36] Of these, biological hydrogels are the easiest to adapt, as they are commercially available, and inherently contain the integrin-binding

and proteolytic domains cells naturally encounter *in vivo*. However, manipulating the concentrations of these proteins in order to control the gel modulus simultaneously alters the density of integrin-binding domains, porosity, and degradability.[22] These parameters cannot be decoupled easily, making it difficult to determine which ECM property most significantly affects cell behavior.

With respect to synthetic hydrogels, PAA was the first popularized platform for cellular mechanobiology,[31] in part because it was the first system to demonstrate independent tuning of cell adhesion and modulus. While PAA is an important material, it has limitations such as a narrow mechanical range, and it is not suitable for three-dimensional (3D) studies. PEG-based gels are inexpensive, have independently tunable cell adhesion, bulk modulus, and proteolytic domains,[11,37,38] and can be used to study cell behavior in 3D.[39–41] However, the mechanical range of PEG-based gels is limited, typically in the range of 0.5-5 kPa when crosslinked with proteolytically degradable groups,[5] or 20-500 kPa with diacrylate or dimethacrylate crosslinking.[11,42] We sought to improve on this limited range of Young's moduli, by combining the commonly used PEG crosslinking with an inexpensive, extremely hydrophilic zwitterion. We report here the synthesis of a hybrid polymer hydrogel, which combines PEG-dimethacrylate (PEGDMA), with the zwitterionic comonomer 2-methacryloyloxyethyl phosphorylcholine (PC). To our knowledge, these "PEG-PC" hydrogels have a mechanical range that matches or exceeds any previously reported hydrogel system, and importantly they are simple and inexpensive to produce, and retain optical clarity over most of the mechanical range.

MATERIALS AND METHODS

2.1. Cell culture

All cells and culture media reagents were purchased from Life Technologies, Carlsbad, CA, unless otherwise noted. Human aortic smooth muscle cells (HASMCs) were cultured in Dulbecco's modified Eagle's medium (DMEM) supplemented with 1% penicillin-streptomycin (P/S) and smooth muscle growth supplement (SMGS). Human hepatocellular carcinoma cells (HEP3Bs, American Type Culture Collection, Manassas, VA), were cultured in modified Eagle's medium (MEM) supplemented with 1% P/S and 10% FBS. Human SkBr3 and MDA-MB-231 (231) breast carcinoma cell lines were generous gifts from Shannon Hughes at the Massachusetts Institute of Technology and Sallie Schneider at the Pioneer Valley Life Sciences Institute, respectively. Both SkBr3 and 231 cell lines were cultured in DMEM supplemented with 1% P/S and 10% FBS.

2.2. Formation of PEG-PC hydrogels

PEG-PC polymer hydrogel precursor solutions were prepared by mixing PEGDMA (average Mn 750, Sigma-Aldrich, St. Louis, MO), varied between final concentrations of 7.4 mM and 0.7 M (0.5-55 wt%, see Figure 1E), and 0.6 M (17 wt%) 2-methacryloyloxyethyl phosphorylcholine (Sigma-Aldrich) in phosphate buffered saline (PBS). Solutions were degassed for 30 seconds with nitrogen, and sterilized with a 0.2 μm syringe filter (Thermo Fisher Scientific, Waltham, MA). Depending on the desired format, two different free radical initiators have been used for polymerization. To cure under UV light, 0.8 wt.% Irgacure 2959 (BASF, Ludwigshafen, Germany) was added, and gel formation was induced with a Spectroline High-Intensity UV Lamp at 365 nm (Model #SB-100P, Westbury, NY), 3.5 inches from the gel for 7 minutes. To

form hydrogels in the absence of UV light, 0.05 wt.% ammonium persulfate (APS) and 0.125 vol.% Tetramethylethylenediamine (TEMED, Bio-Rad Laboratories, Hercules, CA) was added, and gels polymerized under nitrogen for 10 minutes.

To make thin PEG-PC hydrogels with even heights, suitable for microscopy, a 75 μL aliquot of the PEG-PC solution was cured between chemically modified 18 mm glass coverslips. Methacrylate silanized coverslips served as the base, and covalently attached to the hydrogel during polymerization, whereas hydrophobic coverslips could be easily removed from the final, hydrophilic hydrogels. To create the methacrylate coverslips, slips were plasma treated, and subsequently treated with 200 mL of 95% ethanol with 2 vol.% 3-(trimethoxysilyl) propyl methacrylate (adjusted to pH 5.0 with glacial acetic acid; Sigma-Aldrich) for 2 minutes with shaking, washed three times in 100% ethanol, and dried at 120°C for 15 minutes[43]. Hydrophobic coverslips were made with clean cover slips submerged in Sigmacote (Sigma-Aldrich), shaken for 20 minutes, washed 3 times with 100% ethanol, and dried under vacuum. Following polymerization, the Sigmacote cover slips were removed from the gel surface with fine forceps, and the gels were allowed to swell in sterile PBS for 24 hours. Prepared coverslips were stored in foil in a dessicator at room temperature.

To make PEG-PC hydrogels suitable for proliferation experiments, we silanized glass bottom 96-well plates (no. 1.5 coverslip glass; In Vitro Scientific, Sunnyvale, CA) as described above. As a special consideration for the presence of plastic, the plates were dried at 40°C for 30 minutes. Hydrogels were 40 μL in size to fit snugly in each well, and APS was used as the free radical initiator to induce gelation.

2.3. Protein functionalization

To facilitate cell adhesion to the gels, proteins were covalently attached to the hydrogel surfaces. Hydrated gels on coverslips were transferred to 12-well tissue culture dishes and treated twice with sulfo-SANPAH (0.3 mg/mL in pH 8.5 HEPES buffer; ProteoChem, Denver, CO) under UV light for 15 minutes. The gels were washed by twice pipetting sterile PBS directly over the surface and shaking for 10 seconds, followed immediately by incubation with protein cocktails. For gels in 96-well plates, 100 μL of 0.6 mg/mL sulfo-SANPAH was added to each well and the plates exposed to UV light for 20 minutes and then briefly washed three times with HEPES buffer. To demonstrate versatility, we also showed that acrylate-poly(ethylene glycol)-succinimidyl valerate (PEG-SVA; Laysan Bio, Arab, AL) can crosslink proteins by adding it to the PEG-PC pre-hydrogel solution at 0.11 wt.%. This method incorporates an amine reactive group into the bulk of the hydrogel instead of isolating the reaction at the surface.

After reacting the gel surfaces with the heterobifunctional crosslinker, hydrogels presented a highly amine-reactive functional group for covalent linkage to a variety of integrin-binding proteins. We made two different mixtures of integrin-binding proteins (protein "cocktails"), which consisted of either integrin-binding ECM proteins that are found in typical basement membranes (70% collagen III, 15% collagen IV and 15% laminin at 10 $\mu g/cm^2$), or in inflammation and wound healing (50% collagen I and 50% fibronectin at 10 $\mu g/cm^2$). The proteins used were type I collagen (rat tail) and laminin (mouse) (both from Life Technologies), recombinant human collagen III (FibroGen, San Francisco, CA), recombinant human collagen IV (Neuromics, Edina, MN), and human plasma fibronectin (EMD Millipore, Billerica, MA). Protein cocktails were made in sterile PBS and adjusted to pH 3 to prevent collagen gelation.

Post-protein reaction, hydrogels were washed 3x over an hour in sterile PBS with shaking, and then UV sterilized for 60 minutes before cell seeding.

2.4. Hydrogel mechanical and structural characterization

PEG-PC hydrogel cylinders for mechanical compression testing were formed in 5 mm Teflon molds and swelled in PBS for 48 hours. Post-swelling, hydrogel dimensions were measured with digital calipers, and mechanical compression tests were performed with a TA Instruments (New Castle, DE) AR-2000 rheometer at a 2 μm/second strain rate. The Young's modulus (*E*) for each hydrogel was calculated by plotting the measured normal force between 0 and 4% strain, and dividing the slope of the best-fit linear regression by the hydrogel cross-sectional area. The Young's modulus was obtained for 4 or more hydrogels for each PEGDMA concentration.

To determine an approximate average mesh size as a function of PEGDMA crosslinker content with constant PC content, hydrogels were swelled in PBS for 48 hours then weighed, fully lyophilized, and weighed again. The average mesh sizes, ξ, of the PEG-PC hydrogels were determined as a function of PEGDMA crosslinker concentration according to the Flory theory as modified by Canal and Peppas,[44]

$$\xi = \upsilon_{2,s}^{-\frac{1}{3}}(\bar{r}^2)^{1/2}$$

where $\upsilon_{2,s}$ is the swollen volume fraction of polymer and $(\bar{r}^2)^{1/2}$ is the average end-to-end distance of the PEGDMA crosslinker.

To detect unreacted PEG-methacrylate monomers, NMR was performed on PEG-PC samples polymerized with APS and TEMED in microcentrifuge tubes with a Bruker Spectrospin DPX300 (Bruker Corporation, Billerica, MA). D_2O was used as the solvent. To quantitatively measure the observed transparency of PEG-PC versus PEGDMA, hydrogels were made on cover slips, as described above, from 135 mM to 0.7 M PEGDMA with and without 0.6 M PC. After 48 hours of swelling in PBS, the optical densities of hydrogels in clean PBS were measured at 450, 490, 572, 630 and 750 nm with a BioTek ELx800 absorbance microplate reader (BioTek).

2.5. Non-specific protein adsorption quantification

We quantified protein adsorption to the hydrogels with a modified ELISA.[45] Hydrogels were polymerized in 96-well plates, swelled in PBS overnight, and incubated with 10 mg/mL bovine serum albumin (BSA; Sigma) for 20 hours at 37°C. The gels were washed 5x with PBS, and incubated with a primary antibody to BSA (Life Technologies) in PBS for 90 minutes, washed again 5x with PBS, and incubated with secondary antibody conjugated to horseradish peroxidase (HRP; Abcam, Cambridge, UK) for 90 minutes. After washing 5x with PBS, the gels were incubated with 0.1 mg/mL 3,3',5,5'-tetramethylbenzidine (TMB; Sigma) and 0.06% hydrogen peroxide (Fisher) in 0.1 M sodium acetate (pH 5.5; Sigma) for 1 hour at room temperature with shaking. At 1 hour, an equal volume of 1 M sulfuric acid (Sigma) was added to each well, and the absorbance at 450 nm was measured with a BioTek ELx800 absorbance microplate reader (BioTek, Winooski, VT).

2.6. Focal adhesion quantification and imaging

All cell lines were seeded in serum-free DMEM (with the exception of HEP3Bs, which were seeded in MEM) on 18, 26, 165 and 400 kPa PEG-PC hydrogels coupled with 10 μg/cm^2 collagen I. After 48 hours, cells were rinsed 2x with warm PBS, fixed in fresh 4% formaldehyde, and blocked with AbDil (2% BSA in Tris-buffered saline with 0.1% Triton X-100, TBS-T). Vinculin was immunofluorescently labeled with a monoclonal mouse anti-vinculin antibody (Sigma-Aldrich) and an anti-mouse FITC secondary antibody (Jackson ImmunoResearch Laboratories, West Grove, PA). F-actin was fluorescently labeled with Alexa Fluor 555-conjugated phalloidin (Life Technologies), and cell nuclei were labeled with DAPI (MP Biomedicals, Santa Ana, CA). Antibody incubations were performed for 1 hour in AbDil, in the dark, and cells were thoroughly washed between labeling steps with TBS-T. Each sample was equilibrated with ProLong Gold antifade reagent (Life Technologies) for 5 minutes before imaging. Images were taken with a 63x oil immersion lens, on a Zeiss Axio Observer Z1 microscope, and ImageJ (NIH, Bethesda, MD) was used to adjust the brightness and contrast for clarity in figures. With unmodified images, ImageJ's built-in measurement functions were used to quantify focal adhesion area and circularity. A minimum of 42 focal adhesions were manually traced from a minimum of 8 cells per condition.

2.7. Cell Proliferation

In 96-well glass-bottomed plates, PEG-PC hydrogels with Young's moduli of 18, 26, 165 and 400 kPa were polymerized with APS and TEMED. Sulfo-SANPAH was used to attach adhesive proteins (10 μg/cm^2 collagen I) overnight. 231s and SkBr3s were seeded at 6,000 cells/well in serum-free DMEM with 1% P/S; HEP3B cells were seeded at 6,000 cells/well in MEM media with 10% FBS and 1% P/S. In all cases, the media was exchanged for serum-containing media

(10% FBS) 24 hours after seeding. Media was replenished every two days. Five days after seeding, the MTS-based assay CellTiter96 AQueous (Promega, Madison, WI) was added to each well at 20 μL/well to indirectly measure cell proliferation via mitochondrial redox activity. After 4 hours of incubation, the absorbance was read at 490 nm with a BioTek ELx800 absorbance microplate reader. In order to demonstrate how cell number changes as a function of hydrogel modulus, the data is presented as a fold-increase in absorbance compared to the softest (18 kPa) hydrogel tested.

2.8. Statistical Analysis

Statistical analysis was performed using Prism v5.04 (GraphPad Software, La Jolla, CA). Data are reported as mean ± standard deviation, unless otherwise noted. Statistical significance of the difference between pairs of means was evaluated by computing P-values with unpaired Student's t-tests (with Welch's correction as necessary). When one-way ANOVAs were performed, the Tukey post-test was used to determine significance of pairwise differences. $P \leq 0.05$ is denoted with *, ≤ 0.01 with **, ≤ 0.001 with *** and ≤ 0.0001 with ****; $P > 0.05$ is considered not significant ('ns').

RESULTS

3.1. PEG-PC hydrogels are mechanically tunable over a wide range of Young's moduli

We synthesized hydrogels from varying concentrations of PC and PEGDMA, and characterized physical properties important for a viable cell culture platform (Fig. 1). We quantified the Young's moduli of photopolymerized PEG-PC hydrogels with 0.6 M PC (20 wt%) in PBS and PEGDMA ranging from 7.4 to 700 mM (0.5 – 55 wt%) via compression testing (Fig. 1B). As expected, we found increasing hydrogel modulus with increasing crosslinker concentration from 0.9 ± 0.2 kPa at 7.4 mM PEGDMA to 9300 ± 900 kPa at 0.7 M PEGDMA (Fig. 1B). This mechanical characterization represents a hydrogel tunable over four orders of magnitude of Young's moduli, from 900 Pa to nearly 10 MPa. We attribute this wide range of moduli to the inclusion of the PC zwitterion, enabling gelation at very low concentrations of PEGDMA (7.4 mM, or 0.5 wt%). This range of Young's moduli spans the reported moduli of nearly any tissue type, including brain, tumor tissue, skin, cartilage, and some areas of bone.[46]

In the mechanobiology field, laboratories typically use either APS and TEMED or Irgacure as free-radical initiators to induce hydrogel gelation. We observed minor differences in Young's modulus when comparing hydrogels made with one of these two initiators at the same PEGDMA concentration (Suppl. Fig. 1A, B). The Young's modulus of PEG-PC hydrogels at 0.6 M PC and 7.4 mM PEGDMA polymerized with APS was 5.9 kPa, compared to 900 Pa when polymerized with Irgacure. This trend was consistent at low concentrations of PEGDMA. By measuring the gel fractions between each method, we found that the polymerization reaction is less efficient with Irgacure (~13% difference in gelation), resulting in larger mesh sizes, and softer gels (Suppl. Fig. 1B).

FIGURE 1

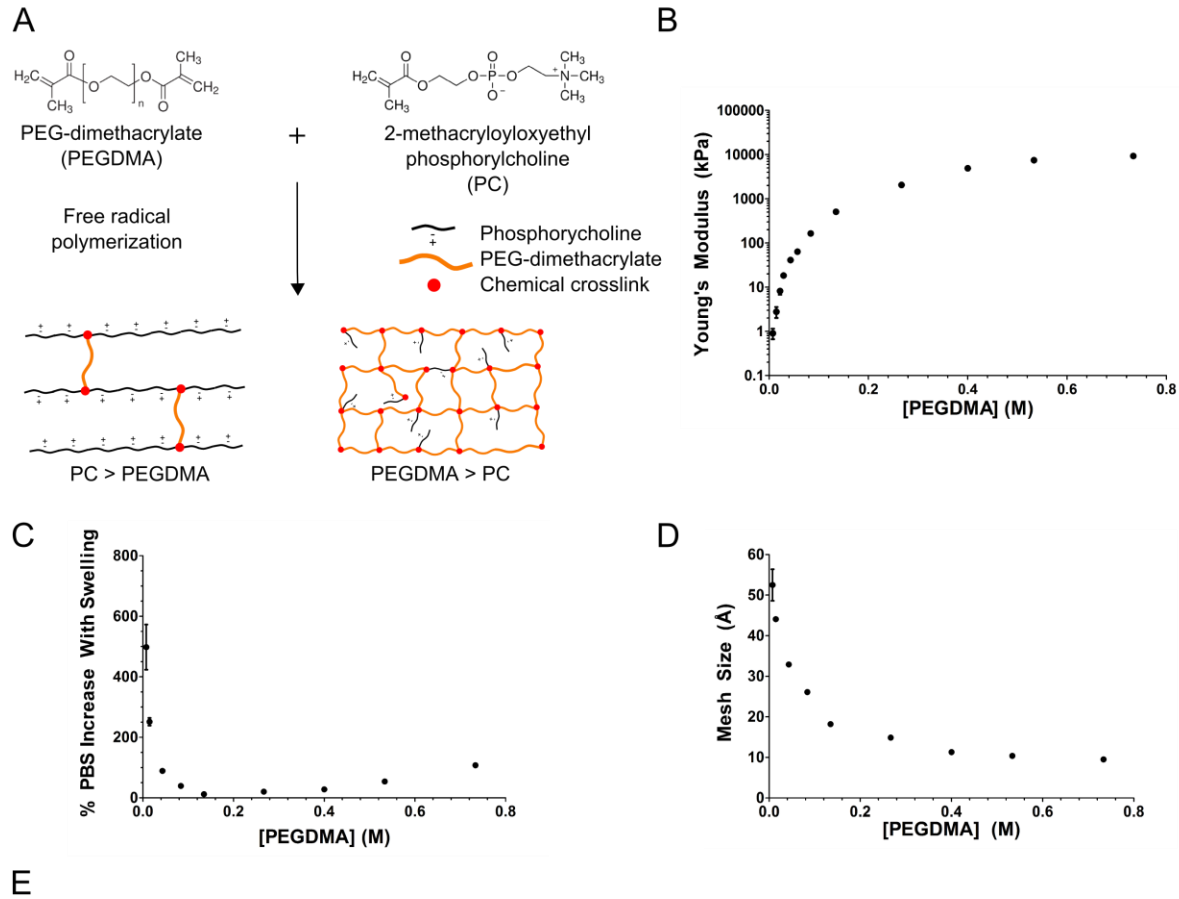

E

[PEGDMA] (M)	0.007	0.015	0.022	0.029	0.043	0.057	0.084	0.135	0.30	0.40	0.50	0.70
[PEGDMA] (wt.%)	0.55	1.1	1.6	2.2	3.2	4.3	6.3	10.1	20	30	40	55
E (kPa)	0.9	2.8	8.2	18	41	64	170	500	2060	4900	7500	9300
SD (kPa)	0.2	0.8	1.5	2.6	5.9	3.7	22	74	66	350	80	920
N	7	6	9	6	6	4	5	8	4	6	3	6

Figure 1: **PEG-PC hydrogels are mechanically tunable over four orders of magnitude in Young's modulus.**

A: Schematic of PEG-PC hydrogel structure. PEG-PC hydrogels were prepared by free-radical polymerization to form PEGDMA-crosslinked linear PC polymers that entangle and form gels at very low crosslinker concentrations. At very high PEGDMA concentrations, the network structure is dominated by PEGDMA with sparsely distributed PCs. B: Young's modulus, *E,* of PEG-PC hydrogels as a function of PEG crosslinker concentration from 7.4 mM to 0.7 M. PC was held at 20 wt% (0.6 M). Error bars are standard deviations. Each adjacent pair is significantly different as determined by an unpaired Student's t-test with $p < 0.001$ or better. C: PEG-PC swelling behavior in PBS, which is maintained at even very high crosslinker concentrations. D. The average mesh sizes of PEG-PC hydrogels (PC at 0.6 M) as a function of PEG crosslinker concentration. Error bars are standard deviations ($N \geq 4$). E. Table detailing all mechanical testing performed.

3.2. PEG-PC hydrogels have small mesh sizes and structure-dependent swelling properties

The average mesh sizes (ξ) of PEG-PC hydrogels from 7.4 mM to 0.7 M PEGDMA ranged from 5.3 ± 0.4 nm at 7.4 mM crosslinker to 0.95 ± 0.01 nm at 0.7 M crosslinker (Fig. 1D). These sizes approximate values reported for other common synthetic hydrogels such as PEG-diacrylate (ξ ~ 1.4 - 7 nm),[47] poly(vinyl alcohol) (ξ ~ 4 - 32 nm),[44] or poly(2-hydroxyethyl methacrylate) (ξ ~ 1.6 - 2.4 nm).[44] While the mesh size of 135 mM PEGDMA hydrogels is only 0.5-fold higher than 135 mM PEG-PC (3.2 nm vs 1.8 nm, respectively), the Young's modulus is 10-fold lower (55 kPa vs 500 kPa, respectively[48]), demonstrating the profound effect of the methacrylic PC polymers (and their impact on the overall gel volume fraction) on the hydrogel mechanical properties.

Interestingly, the expected strong correlation between mesh size and Young's modulus was found only over a partial range of crosslinker concentrations (Fig. 1D). There were two different regimes where mesh size and Young's modulus strongly correlated: from 7.4 to 135 mM PEGDMA (Pearson's R = -0.8383, $p < 0.05$), and from 0.3 to 0.7 M PEGDMA (Pearson's R = -0.9572, $p < 0.05$). Interestingly, these behaviors separate where the weight percent of PC and PEGDMA are equal in the gel. This finding suggests a change in the fundamental structure of the hydrogel, from one dominated by a PEGDMA-crosslinked methacrylic PC polymer to one dominated by a PEGDMA-crosslinked PEG polymer with sparsely distributed PC pendants (Fig. 1A). To investigate whether these regime changes were due to incomplete methacrylate conversion, we collected NMR spectra on the PEG-PC hydrogels. These spectra (Supplementary Figure 2) indicate complete methacrylate conversion for PEG-PC hydrogels up to 0.4M PEGDMA. While it is not possible to directly quantify the methacrylate conversion from these

spectra, the post-swelling dry gel masses for these gels are 99% or more of the theoretical polymer masses (data not shown), implying that methacrylate conversion is very high at all concentrations of PEG.

Given the very high moduli and small mesh sizes of highly crosslinked PEG-PC hydrogels, we speculated that these gels may not swell water typical of PEG gels. Surprisingly, from swelling data, we ascertained that PEG-PC does in fact swell PBS at all crosslinker concentrations (Fig. 1C), and we again observed two different regimes of swelling behavior, separated at the point where the gels undergo a change between a PC and PEG-dominated structure. In examining the stress-strain curves from compression testing, we found that the hydrogels behaved as linear elastic gels at low strain in PC-dominated networks, and non-linearity was observed above this regime change (Supp. Fig. 1C-D). Recent studies have implied that cells may be able to sense these types of differences in network structure.[49] In contrast to these studies, however, we observed non-linearity at only the highest moduli, outside the mechanical range reported to be discernable by most cell types.

3.3 PC groups reduce non-specific protein adsorption to PEG gels

PEG is an amphiphilic polymer that is resistant to non-specific protein adsorption. We hypothesized that incorporation of extremely hydrophilic PC groups would enhance resistance to protein adsorption. We tested this by adsorbing BSA to PEGDMA (0.145 M) and PEG-PC (0.6 M PC, 0.054 M PEGDMA) hydrogels that had the same Young's modulus, and, after extensive washing, measuring the adsorbed protein with a modified ELISA. As we expected, the

PEGDMA hydrogels had small, but detectable levels of BSA on the surface, whereas no BSA was detectable on PEG-PC surfaces (Fig. 2A), nor on polyacrylamide gels (data not shown).

We also quantified the effect of PC content in hydrogels on protein adsorption by measuring BSA adsorption on hydrogels with constant PEGDMA (0.084 M) and varied PC concentration (0.15, 0.3 and 0.6 M). As expected, BSA levels decreased with increasing PC content (Fig. 2B), with half the signal at 0.6 M PC as at 0.15 M. Interestingly, BSA was detected on PEG-PC hydrogels with 0.084 M PEGDMA, but not on the hydrogels with 0.054 M PEGDMA. This suggests that adsorption increases when the ratio of PEGDMA-to-PC increases, further supporting our hypothesis that PC groups decrease non-specific protein adsorption.

3.4. PEG-PC hydrogels are optically transparent

For a hydrogel platform to be particularly useful for microscopy, the optical clarity (and refractive index) would ideally be close to that of glass or plastic substrates. Both PEG and PAA hydrogels become opaque at high crosslinker concentrations. These PEG-PC hydrogels are completely transparent at all but the very highest cross-linker concentrations of (Fig. 2C, D), with opacity emerging when the PEGDMA content reaches 40 wt%. Optical properties were characterized after polymerizing hydrogels on coverslips, then measuring optical density at several different wavelengths (Fig. 2C). PEG-PC hydrogels are completely transparent (having ODs equal to the polystyrene surface) across all wavelengths up to 0.3 M PEGDMA, only becoming opaque at 0.7 M crosslinker. In contrast, PEGDMA-only hydrogels are opaque at lower crosslinker concentrations. At crosslinker concentrations higher than typically used in the

literature, the PEGMDA hydrogels improve their transparency to levels approaching the PEG-PC gels.

FIGURE 2

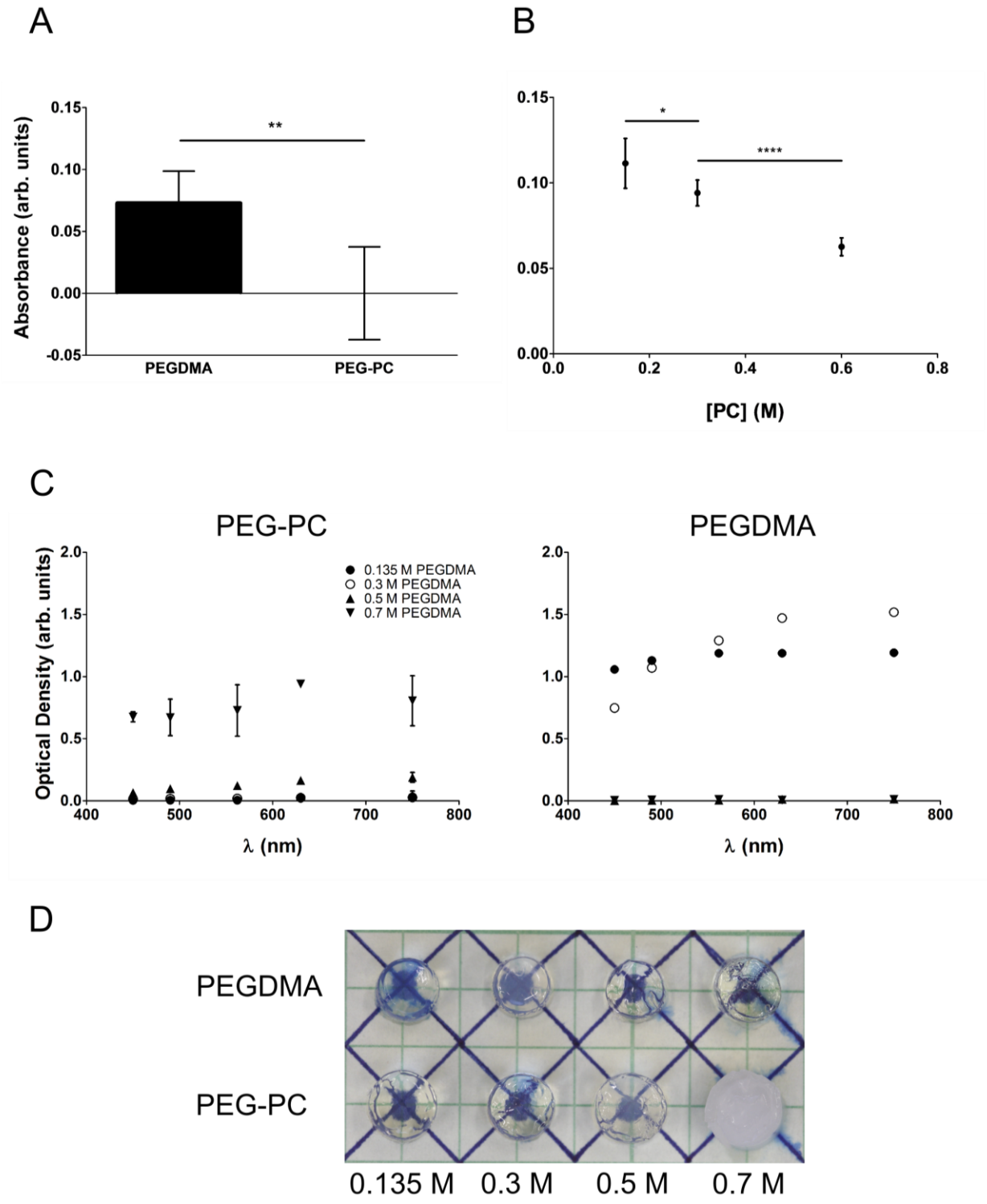

Figure 2: PEG-PC hydrogels are non-fouling, and are optically transparent at low PEGDMA concentrations

A: Comparison of adsorption of BSA to modulus-matched PEGDMA (0.145 M) and PEG-PC (0.6 M PC and 0.054 M PEGDMA) hydrogels measured by ELISA with TMB as detection substrate. No BSA was detected (compared to negative controls) on the PEG-PC hydrogel. B: Adsorbed BSA was measured as a function of PC concentration with constant [PEGDMA] (0.084 M). Adsorption decreases with increasing PC content, demonstrating the ability of PC to prevent fouling. C: The optical density of PEG-PC (left) and PEGDMA (right) hydrogels on coverslips in PBS was measured at several wavelengths. The optical density of PEG-PC hydrogels are lower than PEGDMA hydrogels at 135 mM and 0.3 M, but the opposite is true at 0.5 and 0.7 M. Errors are standard deviations ($N \geq 2$). D: Visual comparison of the optical transparencies of PEG and PEG-PC hydrogels at 0.135, 0.3, 0.5 and 0.7 M PEGDMA. PEG-PC hydrogels are 0.6 M PC.

3.5. PEG-PC hydrogels are suitable for mechanobiology experiments across many cell types

We covalently attached integrin-binding ECM proteins to the surface of PEG-PC hydrogels with two methods: sulfo-SANPAH and PEG-SVA. Both methods enabled cell attachment and spreading on the PEG-PC surfaces (Fig. 3A) with many cell types (Fig. 3B), and different protein mixtures (Fig. 3C). As shown in Fig. 3A, no cell attachment or spreading occurs on PEG-PC surfaces without sulfo-SANPAH or PEG-SVA modification, demonstrating again that these PEG-PC hydrogels are non-fouling, and useful for studies in which parsing the roles of integrin-binding vs. mechanical properties is desired. With coupling, however, extensive cell spreading was observed consistently for all cell types we tested (examples shown are left: smooth muscle, right: liver carcinoma).

FIGURE 3

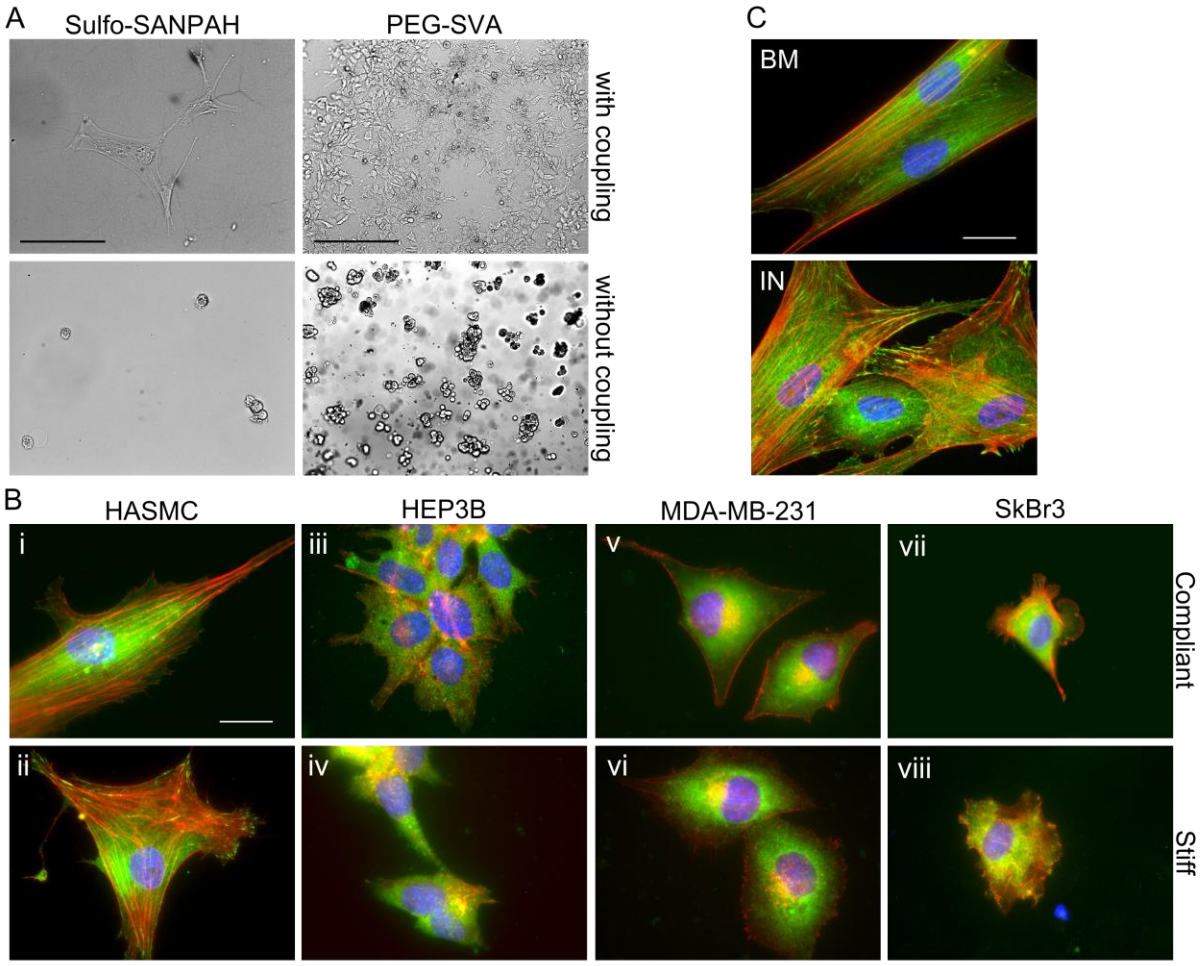

Figure 3: Modulus and integrin-binding on PEG-PC gels controls cell morphology

A: (Left) HASMCs on PEG-PC (84mM PEGDMA) treated with (top) or without (bottom) sulfo-SANPAH and collagen I at 10 μg/cm^2, scale bar is 100 μm. (Right) HEP3B cells on PEG-PC (22 mM PEGDMA) with (top) or without (bottom) PEG-succinimidyl valerate (PEG-SVA) and 65% collagen III, 23% collagen I and 2% fibronectin at 5 μg/cm^2, scale bar is 200 μm. B: i - ii: HASMCs on PEG-PC (compliant = 15 and stiff = 84 mM PEGDMA, 3 and 170 kPa, respectively, except for SkBr3 for which stiff = 0.15 M PEGDMA and 400 kPa) with collagen I. Vinculin = green, F-actin = red, and DNA = blue. iii – iv: HEP3Bs. v - vi: MDA-MB-231s, and vii - viii: SkBr3s. Scale bar is 20 μm. C. HASMCs on basement membrane-like ECM (70% collagen III, 15% each collagen IV and laminin at 10 μg/cm^2 total) and on inflammatory ECM (50% each fibronectin and collagen I at 10 μg/cm^2 total). Scale bar is 20 μm.

Going further, we demonstrated that cells sense differences in the stiffness of PEG-PC hydrogels by performing experiments with three human cell types: liver carcinoma (HEP3B) and two breast cancer cell lines (SkBr3 and MDA-MB-231) (Fig. 3B). After 48 hours of culture on PEG-PC gels of varying stiffness, coupled with 10 μg/cm^2 collagen I, cells were fixed and stained for actin (red), DNA (blue) and vinculin (green). Vinculin staining was used to identify focal adhesions,[50] which were counted and analyzed with ImageJ (Fig. 4A). We manually traced focal adhesions at several stiffness conditions to quantify the number of focal adhesions visible per cell (Fig. 4B), the average focal adhesion area (Fig. 4C) and elongation (Fig. 4D). Focal adhesion circularity was quantified with ImageJ as a measure of adhesion maturity, with elongation (circularity^{-1}) being associated with increased adhesion stability (Fig. 4D).[51]

FIGURE 4

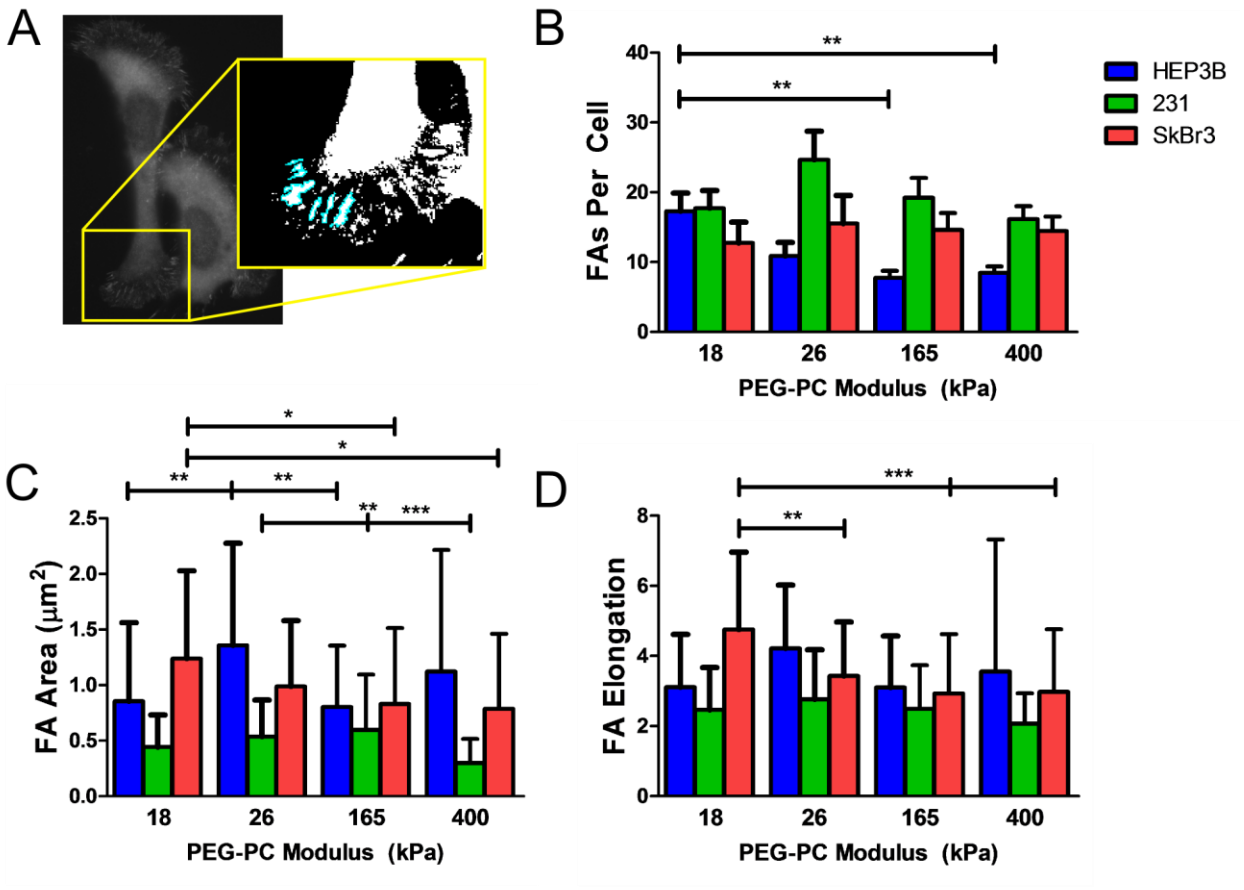

Figure 4: PEG-PC modulus control of focal adhesions is cell-specific

A. Example of image thresholding and focal adhesion tracing performed in ImageJ of an SkBr3 cell with labeled vinculin. B. Average number of focal adhesions (FA) counted per cell as a function of PEG-PC modulus with 10 μg/cm^2 collagen I. HEP3B cells had significantly fewer focal adhesions on the 165 and 400 kPa PEG-PC gels than on the 18 kPa gels, as measured with one-way ANOVA and the Tukey post-test for significance. C. Average focal adhesion area on 18 – 400 kPa PEG-PC with 10 μg/cm^2 collagen I. D. Average focal adhesion elongation (departure from circularity) on 18 – 400 kPa PEG-PC with 10 μg/cm^2 collagen I. SkBr3 focal adhesion elongation decreased by 37% from 18 to 400 kPa.

We observed that focal adhesion area decreased with Young's modulus in SkBr3 and 231 cells (Fig. 4C; areas on the stiffest PEG-PC were reduced approximately 37 and 45% from the softer PEG-PC hydrogels, $p < 0.05$ and $p < 0.01$, respectively), and SkBr3 elongation also decreased

with increasing stiffness. Interestingly, HEP3B focal adhesion area is biphasic (Fig. 4C; area on 26 kPa PEG-PC is 65% larger than on 18 and 165 kPa, $p < 0.01$), and HEP3Bs were the only cell line to have a significant difference in the number of focal adhesions per cell. Both HEP3Bs and MDA-MB-231s had very few cells with actin stress fibers, but many cells had prevalent, actin-rich filopodia (Fig. 3B iii-iv, v-vi). These results demonstrate the ability of PEG-PC hydrogel mechanical properties to tune cytoskeletal organization, and revealed that mechanosensitivity is cell line-specific.

We also synthesized PEG-PC gels at one modulus, while covalently attaching different protein cocktails to regulate integrin-binding to the hydrogel surfaces (Fig. 3C). We cultured HASMCs on a mimic of a basement membrane-like environment (BM: 70% collagen III, 15% collagen IV, and 15% laminin) and an inflammatory environment (IN: 50% collagen I and 50% fibronectin) , and quantified the focal adhesion number, area and elongation. As expected, the number of focal adhesions per cell, adhesion area, and elongation was greater on the inflammatory environment (Suppl. Fig. 3), demonstrating that cells sense differences in ECM proteins on the hydrogels as well as differences in substrate stiffness.

3.6. PEG-PC modulus affects proliferation of multiple cell types

We investigated the role of substrate stiffness on the proliferation of three cell types. HEP3Bs, SkBr3s and 231s were each seeded on PEG-PC gels across a range of modulus with 10 $\mu g/cm^2$ collagen I. We found that 231 proliferation increases by approximately 25-35% (over the reading on 18 kPa hydrogels), for hydrogels between 18 and 26 kPa, before saturating (Fig. 5A). HEP3Bs were most sensitive to substrate modulus, with average proliferation increasing about

60% from 18 kPa to 26 kPa, and then another 60% from 26 kPa to 165 kPa (Fig. 5C). Finally, SkBr3s proliferation *decreased* by 25% between 26 kPa and 165 kPa, and again between 165 kPa and 400 kPa (Fig. 5B).

We connect these proliferation results with our analysis of focal adhesions with simple statistical methods. For instance, HEP3B cells proliferated substantially more on stiff substrates, but they had fewer focal adhesions on these substrates; in contrast, SkBr3 cells proliferated less on the stiffer substrates, with smaller focal adhesions. Finally, 231 cell proliferation increased marginally with stiffness, and their focal adhesions were also minimally affected by substrate modulus. These three contrasting trends imply differing degrees of interconnectedness of adhesion, contractile and proliferation signaling pathways in these cell types. Although the mechanisms of this behavior are outside the scope of this particular study, we quantified the correlations, if any, between focal adhesion number, area, elongation, and cell proliferation for each cell type. Using the Spearman correlation coefficient we find that SkBr3 focal adhesion area and elongation are strongly correlated with proliferation ($R = 1$ and 0.8, respectively), and HEP3B focal adhesion number is inversely correlated with proliferation ($R = -0.8$).

FIGURE 5

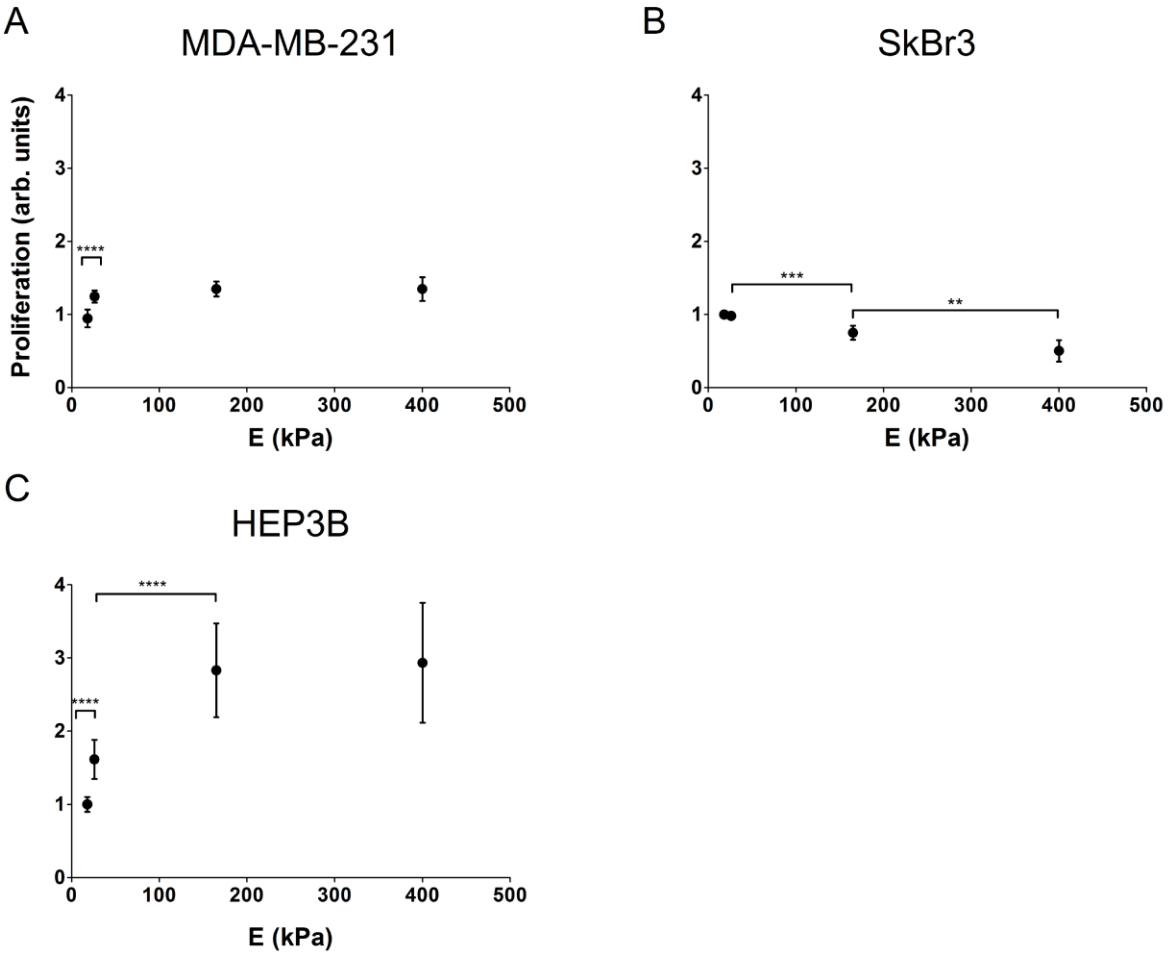

Figure 5: PEG-PC modulus affects cellular proliferation

A: 231, B: SkBr3, and C: HEP3B cells were grown on PEG-PC from 18 to 400 kPa for 5 days and their proliferation quantified with CellTiter96. Results appear as arbitrary absorbance units, which are all related to the internal control of the same cell type on an 18 kPa gel (reported as "1"). 231s and SkBr3s display minor dependence of proliferation on substrate modulus, but with opposing trends. However, HEP3B proliferation is strongly and positively affected by substrate modulus. Error bars are standard error, with N=4, for 231s, N=3 for SkBr3s and N=2 for HEP3Bs.

DISCUSSION

An ideal biomaterial for studying cell-material interactions should be easily tunable across physical properties relevant to the cell type and tissue of interest. Controllable mechanical properties in biomaterials are extremely valuable for understanding cell behavior in heart disease[52,53] and cancer,[54] as cell phenotype[5,7,31] and stem cell differentiation[4,56,57] are sensitive to the modulus of the microenvironment. *In vivo*, a vascular SMC in a healthy arterial media experiences a microenvironment stiffness between 2 and 10 kPa,[58,59] but in an atherosclerotic plaque, the substrate could have stiffness from tens[60,61] to hundreds of kPa.[62] During metastasis, a cancer cell must migrate from a stiff, fibrotic tumor environment through more compliant interstitial tissues and blood vessel walls into the blood stream.[63] Matrix crosslinking and stiffness have profound effects on tumor malignancy[64] and cancer cell metastasis.[63] Other ideal features of hydrogels for mechanobiology include independently tunable stiffness and ligand density, hydrophilicity for reduction of non-specific protein adsorption, and optical clarity for modern quantitative microscopy techniques.

Poly(ethylene glycol) (PEG) is a well characterized amphiphilic polymer widely used as a hydrogel crosslinker in biological applications due to its biocompatibility, mechanical tunability, and anti-fouling properties. However, while it is possible to lower the Young's moduli by adding enzymatic degradation sites to the PEG monomers, PEGDMA hydrogels (Mn 750) cannot polymerize at concentrations $\leq$ 5 wt%, limiting the range of moduli obtainable. Furthermore, PEGDMA hydrogels at most tissue-relevant moduli are opaque (Fig. 2C, D), reducing their attractiveness for high-resolution microscopy.

In the present study, we describe and characterize a new PEG-PC hydrogel that improves upon all these properties. PEG-PC hydrogels are composed of a PEGDMA crosslinker, co-gelled with the PC zwitterion. PC-containing phospholipids are a major component of biological membranes, and PC-polymers exploit biocompatible moieties in synthetic constructs.[65] PC-containing hydrogels and PC-coated surfaces have been exploited for their anti-fouling properties and biocompatibility[65] for use in applications such as contact lenses,[66] cell encapsulation,[67] and drug delivery.[68] There have been two prior reports of a similar polyMPC hydrogel crosslinked with ethylene glycol dimethacrylate and other crosslinkers.[69,70] However, these authors used a much higher concentration of PC (2.5 M versus 0.6 M) and very short crosslinkers in comparison to PEG-PC, and the mechanical properties of the materials were not reported.

Hydrogels which incorporate other zwitterion co-monomers have been studied, in particular sulfobetaines such as 1-(3-sulphopropyl)-2-vinyl-pyridinium-betaine[71,72] and N-(3-sulfopropyl)-N-(methacryloxyethyl)-N,N-dimethylammonium betaine,[73] but not in cell culture contexts. Other routes to hydrophilic hydrogels include hyaluronic acid,[14,16,20,29,74] however, hyaluronic acid is polydisperse, and is known to affect cell behavior through several different cell-surface receptors.[75] PC has the advantages of being inexpensive, and biocompatible without affecting cell behavior, and can be integrated easily into any hydrogel.

We have successfully polymerized PEG-PC hydrogels with as little as 7.4 mM (0.5 wt%) PEGDMA crosslinker up to 0.3 M crosslinker without diminishing optical clarity (Fig. 2C, D). In contrast, PEGDMA hydrogels without PC comonomer cannot polymerize below approximately 70 mM crosslinker, and transparency diminishes at 135 mM crosslinker. Polymerization at such

a low crosslinker concentration imparts PEG-PC hydrogels with a wider range of mechanical properties: the Young's moduli of PEG-PC ranges from 900 Pa at 7.4 mM crosslinker to nearly 10 MPa at 0.7 M crosslinker, which is more compliant at the low end of crosslinker concentration than is possible with PEGDMA hydrogels. This range of stiffnesses is greater than obtainable with PEGDMA gels, and covers a biologically-relevant span that enables reproduction of nearly any biological tissue, e.g. liver (5-55kPa),[76–78] spinal cord (89 kPa), thyroid (9 kPa), breast tumor (4 kPa), carotid artery (90 kPa), and articular cartilage (950 kPa).[46] While bone typically has a modulus from 10-20 GPa,[79] PEG-PC hydrogels with moduli from 1 – 10 MPa may prove useful for studying osteoclasts and other bone-associated cell types. In addition to the exceptional mechanical range and optical properties, we have also demonstrated through BSA adsorption experiments that PEG-PC absorbs less protein than a PEGDMA hydrogel of the same modulus (Fig. 2A), and the amount of adsorbed protein is inversely related to the PC content of the hydrogel (Fig. 2B). These results further confirm the non-fouling properties of PC, which enable a greater degree of control over protein presentation than PEGDMA hydrogels.

From our characterization, we conclude that PEG-PC hydrogels outperform PEG hydrogels as a platform for mechanobiology, and this four order-of-magnitude range of Young's moduli exceeds nearly every previously reported polymer or hydrogel reported for cell culture use, including the recent report of a more tunable version of PDMS.[28] We also discovered that the 135 mM crosslinker hydrogels had mesh sizes half that of a 135 mM PEGDMA gel without PC, whereas the Young's modulus is nearly ten times higher,[48] implying the inherent structural changes outlined in Figure 1. Two reports have demonstrated that hyaluronic acid hydrogels also

have a wide mechanical tunable range,[14,16] however they are more expensive to prepare than PEG-PC gels, require a longer preparation time, and hyaluronic acid has inherent bioactivity that confounds interpretation of results.

The mechanical properties of PEG-PC can be explained by two distinct phenomena at low and high concentrations of crosslinker. At less than 70 mM (5 wt%) crosslinker, PEGDMA does not form a gel. However, integration of the PC polymer allows polymerization with as low as 7.4 mM PEG (0.5 wt%). This is likely due to the overall increase in polymer mass from the PC, which is then crosslinked by the bifunctional PEGs (Fig. 1A). Secondly, although PC is charge neutral in solution due to the intramolecular salt bridge, the PC groups can form dipoles, and it is conceivable that entropic forces (increased water ordering around the PC zwitterions) extend the PEG chains, permitting hydrogel formation at low crosslinker concentration. We have polymerized PEG-PC hydrogels in both water and PBS, and found no differences in the resulting mechanical properties (data not shown), confirming that the mechanical properties of the gels are maintained in the presence of biologically relevant solvents. Regardless of the precise interactions responsible, the resulting hydrogels are far more compliant than with PEGDMA alone, due to the lower overall crosslinking density.

At concentrations of PEGDMA above 135 mM, we observed a large change in the trends of mechanical properties as a function of crosslinker concentration. We hypothesized these effects result from regime changes within the hydrogel, specifically by PEGDMA becoming the dominant hydrogel component, as illustrated in the two extremes of very low and very high PEGDMA concentration in Figure 1A. In this regime, where there is more PEGDMA mass per

volume than PC, the dependency of both mesh size and Young's modulus on crosslinker concentration is much weaker than in the low PEGDMA regime. The ability to form two very different polymer structures with the same two components may largely explain the impressive mechanical range that PEG-PC hydrogels achieve. The structural differences responsible for this transition may be why we consistently observed linear stress-strain curves in the PC > PEGDMA regime and small portions of nonlinearity (up to 1 or 2% strain) in the PEGDMA > PC regime (Supp. Fig 1C, D). This has potential cellular significance due to the recent report that cell phenotype is sensitive to whether a material is linearly elastic or not.[49] However, we could not directly compare results, as we observed non-linearity at low strain in high modulus gels, whereas these authors observed non-linearity at high strain in low modulus gels, implying inherently different networks.

As proof of concept in mechanobiology, we cultured several cell lines (HASMCs, HEP3Bs, and several breast cancer cell lines: SkBr3 and 231 shown here, BT-549 and others not shown) on PEG-PC gels from 3 to 400 kPa Young's moduli functionalized with collagen I, and quantified the effect of substrate stiffness on cell morphology and focal adhesion number, size and elongation. The relationship between focal adhesion properties and substrate modulus was cell type-dependent (Fig. 4), as was the relation between focal adhesion properties and proliferation. Mechanobiology reports with these cell lines is limited, but one report on the 231s showed a decrease in relative adhesivity with increasing stiffness.[80] This report is supported by our findings that focal adhesion area decreases with stiffness, but a direct comparison cannot be drawn due to experimental differences. Comparing our focal adhesion quantification with proliferation has revealed cell type-specific differences in mechanotransduction. These different

trends highlight how cell type-specific differences in mechanotransduction machinery reported elsewhere (integrins, adhesion proteins, actin, myosin and many more)[81,82] can result in very different mechanosensing properties and subsequent changes in pathway signaling. Previously available mechanotransduction data on these cell lines is limited, and our results may guide future research. We propose that PEG-PC hydrogels are ideal for these, and similar studies.

CONCLUSIONS

We have developed a new class of hydrogels by combining the tunability and versatility of PEG hydrogels with biomimetic comonomer, PC. These hydrogels have an extremely wide range of mechanical properties, with the additional advantages of being inexpensive, simple to synthesize, and optically clear. PEG-PC gels can be used to study mechanobiology across many different cell types, and we encourage others to adapt this system to study cellular responses to ECM modulus.

ACKNOWLEDGEMENTS

This work was supported by a generous start-up package from the University of Massachusetts Amherst, and the National Science Foundation Materials Research Science and Engineering Center on Polymers at UMass (DMR-0820506) to S.R.P. S.R.P. and T.V.N. were partially supported by a Barry and Afsaneh Siadat Career Development Award. T.S.E. was partially supported by NIH-R21 (CA167674). W.G.H. was supported by a fellowship from the Institute of Cellular Engineering IGERT at UMass. S.M. was supported through a Graduate Research Fellowship from the National Science Foundation. We are thankful to the UMass MRSEC for use of the core rheometer, and Aaron Chen for assistance with photography. We thank Prof. Gregory Tew for helpful intellectual discussions.

SUPPORTING INFORMATION

We include two supplementary figures. Supplemental Figure 1 includes further characterization of the PEG-PC hydrogels, including Young's modulus data for PEG-PC hydrogels polymerized with APS and TEMED (Suppl. Fig. 1A), a table summarizing the comparison between gel

formation between APS/TEMED and Irgacure (Suppl. Fig. 1B), and representative stress-strain plots depicting the linear and non-linear elastic properties of the gels (C-D). Supplemental Figure 2 shows the NMR spectra for PEG-PC hydrogels with varying PEGDMA crosslinker. Supplemental Figure 3 shows focal adhesion quantification of cells cultured on hydrogels of the same modulus, comparing between the inflammatory protein mixture and the basement membrane mixture.

REFERENCES

(1) Lo, C. M.; Wang, H. B.; Dembo, M.; Wang, Y. L. *Biophys. J.* **2000**, *79*, 144–152.

(2) Wong, J. Y.; Velasco, A.; Rajagopalan, P.; Pham, Q. *Langmuir* **2003**, *19*, 1908–1913.

(3) Peyton, S. R.; Putnam, A. J. *J. Cell. Physiol.* **2005**, *204*, 198–209.

(4) Engler, A. J.; Sen, S.; Sweeney, H. L.; Discher, D. E. *Cell* **2006**, *126*, 677–89.

(5) Peyton, S. R.; Kim, P. D.; Ghajar, C. M.; Seliktar, D.; Putnam, A. J. *Biomaterials* **2008**, *29*, 2597–607.

(6) Saha, K.; Keung, A. J.; Irwin, E. F.; Li, Y.; Little, L.; Schaffer, D. V; Healy, K. E. *Biophys. J.* **2008**, *95*, 4426–38.

(7) Engler, A. J.; Griffin, M. A.; Sen, S.; Bonnemann, C. G.; Sweeney, H. L.; Discher, D. E. *J. Cell Biol.* **2004**, *166*, 877–887.

(8) Peyton, S. R.; Ghajar, C. M.; Khatiwala, C. B.; Putnam, A. J. *Cell Biochem. Biophys.* **2007**, *47*, 300–320.

(9) Orr, A. W.; Helmke, B. P.; Blackman, B. R.; Schwartz, M. A. *Dev. Cell* **2006**, *10*, 11–20.

(10) Nuttelman, C. R.; Mortisen, D. J.; Henry, S. M.; Anseth, K. S. *J. Biomed. Mater. Res.* **2001**, *57*, 217–23.

(11) Peyton, S. R.; Raub, C. B.; Keschrumrus, V. P.; Putnam, A. J. *Biomaterials* **2006**, *27*, 4881–93.

(12) Adelöw, C.; Segura, T.; Hubbell, J. a; Frey, P. *Biomaterials* **2008**, *29*, 314–26.

(13) Ouasti, S.; Donno, R.; Cellesi, F.; Sherratt, M. J.; Terenghi, G.; Tirelli, N. *Biomaterials* **2011**, *32*, 6456–70.

(14) Ananthanarayanan, B.; Kim, Y.; Kumar, S. *Biomaterials* **2011**, *32*, 7913–23.

(15) Weng, S.; Fu, J. *Biomaterials* **2011**, *32*, 9584–93.

(16) Marklein, R. A.; Burdick, J. A. *Soft Matter* **2010**, *6*, 136.

(17) Diener, A.; Nebe, B.; Lüthen, F.; Becker, P.; Beck, U.; Neumann, H. G.; Rychly, J. *Biomaterials* **2005**, *26*, 383–92.

(18) Brown, X. Q.; Ookawa, K.; Wong, J. Y. *Biomaterials* **2005**, *26*, 3123–9.

(19) Leipzig, N. D.; Shoichet, M. S. *Biomaterials* **2009**, *30*, 6867–78.

(20) Khetan, S.; Guvendiren, M.; Legant, W. R.; Cohen, D. M.; Chen, C. S.; Burdick, J. A. *Nat. Mater.* **2013**, *12*, 1–8.

(21) Raeber, G. P.; Lutolf, M. P.; Hubbell, J. a *Biophys. J.* **2005**, *89*, 1374–88.

(22) Zaman, M. H.; Trapani, L. M.; Sieminski, A. L.; Mackellar, D.; Gong, H.; Kamm, R. D.; Wells, A.; Lauffenburger, D. A.; Matsudaira, P.; Siemeski, A. *Proc. Natl. Acad. Sci. U. S. A.* **2006**, *103*, 10889–10894.

(23) Munoz-Pinto, D. J.; Bulick, A. S.; Hahn, M. S. *J Biomed Mater Res A* **2009**, *90*, 303–16.

(24) Winer, J. P.; Janmey, P. a; McCormick, M. E.; Funaki, M. *Tissue Eng., Part A* **2009**, *15*, 147–54.

(25) Brown, X. Q.; Bartolak-Suki, E.; Williams, C.; Walker, M. L.; Weaver, V. M.; Wong, J. Y. *J. Cell. Physiol.* **2010**, *225*, 115–22.

(26) Hartman, O.; Zhang, C.; Adams, E. L.; Farach-Carson, M. C.; Petrelli, N. J.; Chase, B. D.; Rabolt, J. F. *Biomacromolecules* **2009**, *10*, 2019–32.

(27) Browning, M. B.; Wilems, T.; Hahn, M.; Cosgriff-Hernandez, E. *J. Biomed. Mater. Res. A* **2011**, *98*, 268–73.

(28) Palchesko, R. N.; Zhang, L.; Sun, Y.; Feinberg, A. W. *PLoS One* **2012**, *7*, e51499.

(29) Rehfeldt, F.; Brown, A. E. X.; Raab, M.; Cai, S.; Zajac, A. L.; Zemel, A.; Discher, D. E. *Integr. Biol.* **2012**, *4*, 422–30.

(30) Pelham, R. J.; Wang, Y.-L. *Proc. Natl. Acad. Sci. U. S. A.* **1997**, *94*, 13661–13665.

(31) Pelham Jr., R. J.; Wang, Y. L. *Biol. Bull.* **1998**, *194*, 348–350.

(32) Engler, A.; Bacakova, L.; Newman, C.; Hategan, A.; Griffin, M.; Discher, D. *Biophys. J.* **2004**, *86*, 617–28.

(33) Rowley, J. A.; Madlambayan, G.; Mooney, D. J. *Biomaterials* **1999**, *20*, 45–53.

(34) Deroanne, C. F.; Lapiere, C. M.; Nusgens, B. V *Cardiovasc. Res.* **2001**, *49*, 647–658.

(35) Ghajar, C. M.; Chen, X.; Harris, J. W.; Suresh, V.; Hughes, C. C. W.; Jeon, N. L.; Putnam, A. J.; George, S. C. *Biophys. J.* **2008**, *94*, 1930–41.

(36) Wozniak, M. A.; Desai, R.; Solski, P. A.; Der, C. J.; Keely, P. J. *J. Cell Biol.* **2003**, *163*, 583–595.

(37) Hern, D. L.; Hubbell, J. A. *J. Biomed. Mater. Res.* **1998**, *39*, 266–276.

(38) Bryant, S. J.; Anseth, K. S. *J Biomed Mater Res A* **2003**, *64*, 70–79.

(39) Stachowiak, A. N.; Irvine, D. J. *J. Biomed. Mater. Res.* **2008**, *85*, 815–828.

(40) Lee, S.-H.; Moon, J. J.; Miller, J. S.; West, J. L. *Biomaterials* **2007**, *28*, 3163–3170.

(41) Gonen-Wadmany, M.; Oss-Ronen, L.; Seliktar, D. *Biomaterials* **2007**, *28*, 3876–3886.

(42) Temenoff, J. S.; Athanasiou, K. A.; LeBaron, R. G.; Mikos, A. G. *J. Biomed. Mater. Res.* **2002**, *59*, 429–437.

(43) Liu, V. A.; Bhatia, S. N. *Biomed. Microdevices* **2002**, *4*, 257–266.

(44) Canal, T.; Peppas, N. A. *J. Biomed. Mater. Res. A* **1989**, *23*, 1183–1193.

(45) Chang, Y.; Cheng, T.; Shih, Y.; Lee, K.; Lai, J. *J. Membr. Sci.* **2008**, *323*, 77–84.

(46) Levental, I.; Georges, P. C.; Janmey, P. A. *Soft Matter* **2007**, *3*, 299.

(47) Cruise, G. M.; Scharp, D. S.; Hubbell, J. A. *Biomaterials* **1998**, *19*, 1287–94.

(48) Peyton, S. R.; Kalcioglu, Z. I.; Cohen, J. C.; Runkle, A. P.; Van Vliet, K. J.; Lauffenburger, D. A.; Griffith, L. G. *Biotechnol. Bioeng.* **2011**, *108*, 1181–93.

(49) Winer, J. P.; Oake, S.; Janmey, P. a *PLoS One* **2009**, *4*, e6382.

(50) Geiger, B.; Tokuyasu, K. T.; Dutton, A. H.; Singer, S. J. *Proc. Natl. Acad. Sci. U. S. A.* **1980**, *77*, 4127–31.

(51) Zaidel-Bar, R.; Cohen, M.; Addadi, L.; Geiger, B. *Biochem. Soc. Trans.* **2004**, *32*, 416–420.

(52) Laurent, S.; Boutouyrie, P.; Lacolley, P. *Hypertension* **2005**, *45*, 1050–5.

(53) Hahn, C.; Schwartz, M. A. *Nat. Rev. Mol. Cell Biol.* **2009**, *10*, 53–62.

(54) Makale, M. *Birth Defects Res., Part C* **2007**, *81*, 329–43.

(55) Thakar, R. G.; Cheng, Q.; Patel, S.; Chu, J.; Nasir, M.; Liepmann, D.; Komvopoulos, K.; Li, S. *Biophys. J.* **2009**, *96*, 3423–32.

(56) Du, J.; Chen, X.; Liang, X.; Zhang, G.; Xu, J.; He, L.; Zhan, Q.; Feng, X. *Proc. Natl. Acad. Sci. U. S. A.* **2011**, *108*, 9466–9471.

(57) Park, J. S.; Chu, J. S.; Tsou, A. D.; Diop, R.; Tang, Z.; Wang, A.; Li, S. *Biomaterials* **2011**, *32*, 3921–30.

(58) Engler, A. J. A. J.; Richert, L.; Wong, J. Y.; Picart, C.; Discher, D. E. D. E. *Surf. Sci.* **2004**, *570*, 142–154.

(59) Peloquin, J.; Huynh, J.; Williams, R. M.; Reinhart-King, C. A. *J. Biomech.* **2011**, *44*, 815–21.

(60) Tracqui, P.; Broisat, A.; Toczek, J.; Mesnier, N.; Ohayon, J.; Riou, L. *J. Struct. Biol.* **2011**, *174*, 115–23.

(61) Moriwaki, T.; Oie, T.; Takamizawa, K.; Murayama, Y.; Fukuda, T.; Omata, S.; Kanda, K.; Nakayama, Y. *J. Artif. Organs* **2011**, *14*, 276–283.

(62) Fung, Y. C. *Biomechanics: Mechanical Properties of Living Tissues*; 2nd ed.; Springer, 1993.

(63) Kumar, S.; Weaver, V. M. *Cancer Metastasis Rev.* **2009**, *28*, 113–27.

(64) Levental, K. R.; Yu, H.; Kass, L.; Lakins, J. N.; Egeblad, M.; Erler, J. T.; Fong, S. F. T.; Csiszar, K.; Giaccia, A.; Weninger, W.; Yamauchi, M.; Gasser, D. L.; Weaver, V. M. *Cell* **2009**, *139*, 891–906.

(65) Lewis, A. *Colloids Surf., B* **2000**, *18*, 261–275.

(66) Shimizu, T.; Goda, T.; Minoura, N.; Takai, M.; Ishihara, K. *Biomaterials* **2010**, *31*, 3274–80.

(67) Xu, Y.; Jang, K.; Konno, T.; Ishihara, K.; Mawatari, K.; Kitamori, T. *Biomaterials* **2010**, *31*, 8839–46.

(68) Chen, X.; McRae, S.; Parelkar, S.; Emrick, T. *Bioconjugate chem.* **2009**, *20*, 2331–41.

(69) Kiritoshi, Y.; Ishihara, K. *J. Biomater. Sci., Polym. Ed.* **2002**, *13*, 213–24.

(70) Kiritoshi, Y.; Ishihara, K. *Polymer (Guildf)* **2004**, *45*, 7499–7504.

(71) Xue, W.; Huglin, M. B.; Liao, B. *Eur. Polym. J.* **2006**, *42*, 3015–3023.

(72) Xue, W.; Huglin, M. B.; Liao, B.; Jones, T. G. J. *Eur. Polym. J.* **2007**, *43*, 915–927.

(73) Zhang, Z.; Chao, T.; Jiang, S. *J. Phys. Chem. B* **2008**, *112*, 5327–32.

(74) Young, J. L.; Engler, A. J. *Biomaterials* **2011**, *32*, 1002–9.

(75) Necas, J.; Bartosikova, L.; Brauner, P.; Kolar, J. *Vet. Med. (Prague, Czech Repub.)* **2008**, *53*, 397–411.

(76) Masuzaki, R.; Tateishi, R.; Yoshida, H.; Sato, T.; Ohki, T.; Goto, T.; Sato, S.; Sugioka, Y.; Ikeda, H.; Shiina, S.; Kawabe, T.; Omata, M. *Hepatol. Int.* **2007**, *1*, 394–7.

(77) Ganne-Carrié, N.; Ziol, M.; De Ledinghen, V.; Douvin, C.; Marcellin, P.; Castera, L.; Dhumeaux, D.; Trinchet, J.-C.; Beaugrand, M. *Hepatology (Baltimore, MD, U. S.)* **2006**, *44*, 1511–7.

(78) Vizzutti, F.; Arena, U.; Romanelli, R. G.; Rega, L.; Foschi, M.; Colagrande, S.; Petrarca, A.; Moscarella, S.; Belli, G.; Zignego, A. L.; Marra, F.; Laffi, G.; Pinzani, M. *Hepatology (Baltimore, MD, U. S.)* **2007**, *45*, 1290–7.

(79) Rho, J. Y.; Kuhn-Spearing, L.; Zioupos, P. *Med. Eng. Phys.* **1998**, *20*, 92–102.

(80) Tilghman, R. W.; Cowan, C. R.; Mih, J. D.; Koryakina, Y.; Gioeli, D.; Slack-Davis, J. K.; Blackman, B. R.; Tschumperlin, D. J.; Parsons, J. T. *PLoS One* **2010**, *5*, e12905.

(81) Mostafavi-Pour, Z.; Askari, J. a; Parkinson, S. J.; Parker, P. J.; Ng, T. T. C.; Humphries, M. J. *J. Cell Biol.* **2003**, *161*, 155–67.

(82) Georges, P. C.; Janmey, P. A. *J. Appl. Physiol.* **2005**, *98*, 1547–53.